



Bispecific VEGF-A and Angiopoietin-2 Antagonist RO-101 Preclinical Efficacy in Model of Neovascular Eye Disease

Li Xu, PhD,¹ Jessi R. Prentice, MSN,² Raul Velez-Montoya, MD,³ Alina Sinha, BA,⁴ Mark R. Barakat, MD,⁵ Ashwin Gupta, BS,⁶ Robert Lowenthal, MD,² Arshad M. Khanani, MD,⁷ Peter K. Kaiser, MD,⁸ Jeffrey S. Heier, MD,⁹ Anthony Jones, DO,¹⁰ Joshua L. Morgenstern, BA,¹⁰ Anne Strong Caldwell, MD,¹⁰ Niklaus Mueller, PhD,¹⁰ Hugo Quiroz-Mercado, MD,³ Michael Huward, MD,¹¹ Jeffrey L. Olson, MD,¹⁰ Ramesh Bhatt, PhD,¹ Ramanath Bhandari, MD²

Objective: To investigate preclinical data regarding the efficacy and biocompatibility of a bispecific protein, RO-101, with effects on VEGF-A and angiopoietin-2 (Ang-2) for use in retinal diseases.

Design: Experimental study.

Subjects: Brown Norway rats and New Zealand White Cross rabbits.

Methods: Preclinical study data of RO-101 in terms of target-specific enzyme-linked immunosorbent assay binding affinity to VEGF-A and Ang-2, vitreous half-life, inhibition of target-receptor interaction, laser choroidal neovascular membrane animal model, human umbilical vein endothelial cell migration, and biocompatibility was obtained. Where applicable, study data were compared with other anti-VEGF agents.

Main Outcome Measures: Binding affinity, half-life, biocompatibility, and efficacy of RO-101. Neovascularization prevention by RO-101.

Results: RO-101 demonstrated a strong binding affinity for VEGF-A and Ang-2 and in vitro was able to inhibit binding to the receptor with higher affinity than faricimab. The half-life of RO-101 is comparable to or longer than current VEGF inhibitors used in retinal disease. RO-101 was found to be biocompatible with retinal tissue in Brown Norway rats. RO-101 was as effective or more effective than current anti-VEGF therapeutics in causing regression of neovascular growth in vivo.

Conclusions: RO-101 is a promising candidate for use in retinal diseases. In preclinical models, RO-101 demonstrated similar or higher regression of neovascular growth to current anti-VEGF therapeutics with comparable or longer half-life. It also demonstrates a strong binding affinity for VEGF-A and Ang-2. It also was shown to be biocompatible with retinal tissue in animal studies, indicating potential compatibility for use in humans.

Financial Disclosure(s): Proprietary or commercial disclosure may be found in the Footnotes and Disclosures at the end of this article. *Ophthalmology Science* 2024;4:100467 © 2024 by the American Academy of Ophthalmology. This is an open access article under the CC BY-NC-ND license (<http://creativecommons.org/licenses/by-nc-nd/4.0/>).

Choroidal neovascularization, with its resulting vascular leakage, bleeding, and scarring, is the hallmark of exudative age-related macular degeneration (eAMD) and leads to vision loss.¹ VEGF has been thought to play an important role in eAMD by inducing angiogenesis and microvascular leakage. This has been supported by several lines of evidence demonstrating VEGF expression in choroidal neovascular membranes (CNVM) of patients with AMD.^{2,3} Studies have also revealed increased retinal and vitreous VEGF levels in patients and animals with ischemic retinopathies.^{4,5}

Anti-VEGF antibodies, antibody fragments, and receptor decoys have been shown to reduce neovascularization and vessel permeability in a primate model of choroidal vascularization.⁶ Prevention of neovascularization in diseases such as eAMD, diabetic retinopathy, and retinal vein occlusion is currently targeted at inhibiting VEGF binding

and signaling through its cognate receptor, thus reducing neovascularization.^{7,8} Current intravitreal anti-VEGF therapies for retinal diseases include bevacizumab, ranibizumab, aflibercept, brolucizumab, and faricimab. Of these therapies, the recently approved bispecific antibody faricimab uniquely targets both VEGF-A and angiopoietin-2 (Ang-2).⁹

Angiopoietin-2 has been shown to promote vascular leakage and abnormal vessel structure by inactivation of the TIE2 receptor.¹⁰ In ischemic retina models, coexpression of Ang-2 with VEGF-A has shown accelerated neovascularization compared with VEGF-A alone.^{11,12} Reports of elevated VEGF-A and Ang-2 levels in vitreous samples from diabetic patients undergoing vitrectomy were correlated with increased disease severity.^{13,14}

VEGF-A monotherapy has been the mainstay of treatment for retinal neovascular diseases for the last decade and the

efficacy of anti-VEGF therapy has been validated in numerous phase III studies.^{15–18} However, a subset of patients do not respond to treatment with VEGF-A monotherapy and demonstrate little to no reduction in retinal fluid after treatment. Up to 45% of the eAMD population were shown to be “non-responders” or “poor-responders” and as such have a high injection burden with worse visual outcomes.¹⁹ The ability to bind 2 targets simultaneously may result in better disease control and durability, especially in this subset of VEGF-A nonresponders. Indeed, the phase II Ruby Trial showed improved CST in patients cotreated with aflibercept and high-dose nesvacumab (anti-Ang-2 antibody) compared with aflibercept alone.²⁰

We show that RO-101, a bispecific targeting both VEGF-A and Ang-2, has the potential to provide therapeutic results equal to or better than current standards of treatment for eAMD, especially among nonresponders or suboptimal responders to current therapies. The purpose of this study was to establish the efficacy and biocompatibility of RO-101 in relevant experimental *in vivo* models.

Methods

Transient RO-101 Protein Production

The pTT5-based expression vector (Canadian National Research Center) was used for transient gene expression. The codon-optimized surrogate light chain (SLC) gene, anti-VEGF, and anti-Ang-2 heavy chain (HC) genes were cloned into pTT5 vector via 5' restriction site EcoR I and 3' restriction site Not I, respectively. Each gene expression plasmid contained a Kozak sequence and a signal sequence. For transient transfection, the FreeStyle 293-F Cells (HEK293-F, Invitrogen) were cultured and maintained at 37° C in an 8% CO₂ humidified incubator with a shaker platform at 125 rpm as per the manufacturer's instruction. The HEK293-F cells were seeded to a 1-liter flask in 250 ml culture scale per flask the day before transfection. After overnight growth, the cells were counted. For a 250 ml cell transfection, a mix of 125 µg pTT5-SLC, 62.5 µg pTT5-anti-VEGF-HC, and 62.5 µg pTT5-anti-Ang-2-HC plasmids was added to the medium. The DNA mixture was then mixed with 250 µg of 2 mg/ml sterile polyethylenimine in the medium (linear, 25 kDa) (Polysciences #23966, prepared in phosphate balanced saline [PBS]). After 15 minutes of incubation at room temperature, the DNA-polyethylenimine complex mixtures were added to the cells in a flask containing 250 ml growth medium. The transfected cells were grown at 37° C in an 8% CO₂ humidified incubator with a shaker platform at 125 rpm. Sixteen to 24 hours posttransfection, the transfected cells were supplemented with Tryptone TN1 (TekniScience Inc #19553) to a final concentration of 0.5% (diluted from 20% solution made in growth medium) and allowed to grow at 37° C in an 8% CO₂ humidified incubator with a shaker platform at 125 rpm. Six days posttransfection, cell supernatants were harvested by 2 centrifugations to remove cell pellets. The supernatants were then filtered through a 0.2-µm filter unit and ready for protein A purification. The harvested supernatants resulting from transient transfections were purified by rProtein A GraviTrap (GE 28-9852-55), as per GE's instruction. The purified proteins then were desalted using Amicon Ultra-15 Ultracel–MW 100K (Millipore, Cat. No. UFC910024) and sterilized by 0.22 µm syringe filter unit. The final buffer was PBS, and the concentration was determined by absorbance at 280 nm. The purified proteins were qualified in SEC analysis using Tosoh TSKgel BioAssist G3SWxl, and in sodium dodecyl-sulfate

polyacrylamide gel electrophoresis under nonreducing and reducing conditions.

Stable RO-101 Protein Production

The gene expression plasmids used for generating stable cell lines were constructed by Lonza using Lonza's proprietary multi-gene vector system. Three types of expression plasmids were generated using pXC-TGV and pXC-QGV, respectively. The pXC-TGV-based expression plasmid contained 1 copy of the SLC gene, 1 copy of anti-VEGF HC, and 1 copy of anti-Ang-2 HC (TGV). The pXC-QGV-based expression plasmid contained 2 copies of the SLC gene, 1 copy of anti-VEGF HC, and 1 copy of anti-Ang-2 HC (QGV1 and QGV2). The establishment of the RO-101-expressed stable CHOK1SV GS-KO cell line was carried out by Lonza. DNA plasmids were transfected to cells via electroporation using the Gene Pulse XCell. For each transfection, 100 µl linearized DNA at a concentration of 400 µg/ml was aliquoted into a 0.4 cm gap electroporation cuvette, and a 700 µl cell suspension was added. Three cuvettes of cells and DNA were electroporated at 300 V, 900 µF and immediately transferred to 30 ml of prewarmed CD-CHO, supplemented with 10 ml/l SP4 (Lonza, BESPI076E), to generate a stable pool. The transfectants were incubated in a shaking incubator at 36.5° C, 5% CO₂, 85% humidity, 140 rpm. Twenty-four hours posttransfection, the cultures were centrifuged and resuspended into prewarmed CD-CHO, supplemented with 50 µM MSX (L-methionine sulfoximine, Sigma-Aldrich, M5379) and 10 ml/l SP4. Subsequently, the stable recombinant CHOK1 SV GS-KO cells were cultured in CD-CHO media supplemented with MSX and SP4. Transfected cells were routinely subcultured every 3 to 4 days, seeding at 0.2 × 10⁶ cells/ml, and propagated. The clarified cell culture supernatant was analyzed on an Octet R8 using Protein A Biosensors (ForteBio, 18-5010) for expressed proteins. The clarified supernatants generated from the stable pool cultures were purified using an in-house packed 100 ml HiTrap MabSelect SuRE column (Cytiva) on an AKTA purifier at 20 ml/min (Lonza). The column was equilibrated with 50 mM sodium phosphate, 125 mM sodium chloride (pH 7.0), washed with 50 mM sodium phosphate, and 1 M sodium chloride (pH 7.0) followed by reintroduction of equilibration before elution. The molecule was eluted with 10 mM sodium formate (pH 3.5). Eluted fractions were immediately pH-adjusted by neutralizing with 10x PBS buffer (pH 7.4) and titrated to an approximate pH of 7.2 by the addition of dilute sodium hydroxide solution. A further polishing step was performed to reduce soluble aggregate levels using a proprietary Lonza method. The product was applied at a ratio of a maximum of 25 mg per ml of resin. The protein was eluted with a salt gradient and eluted fractions were analyzed by size exclusion-high-performance liquid chromatography, before proceeding to pool selected fractions. The pooled material was analyzed by size exclusion-high-performance liquid chromatography and reduced and nonreduced sodium dodecyl-sulfate polyacrylamide gel electrophoresis.

Vitreous Half-Life

All experiments involving animal models were conducted with the approval of, and under compliance with standards set by, the local institutional animal care and use committee. Anesthesia of New Zealand White Cross rabbits was achieved via intramuscular injection of a suspension of ketamine (10 mg/kg) and xylazine (3 mg/kg). Eyes were dilated using a drop of a 2.5% phenylephrine-HCl/1% tropicamide solution. Methylcellulose gel 1% was placed topically to prevent corneal dehydration.

Once the rabbits were properly anesthetized, a measurement of vitreous RO-101 levels was performed with an ocular

fluorophotometer (OcuMetrics) before injection of fluorescein-labeled RO-101 (concentration 0.3 $\mu\text{g/ml}$), and postinjection readings done at 15 minutes, 30 minutes, 1 hour, and 12 hours. All animals were warmed on a heating pad until full recovery was observed. Recordings of the vitreous fluorescence were made for each eye by scanning anterior to the retina and posterior to the crystalline lens. Background fluorescence of the vitreous was determined for each eye before intravitreal injection. The fluorescence intensity due to fluorescein-labeled RO-101 was measured after the intravitreal injection. Determination of the vitreous fluorescence was made by averaging the values around the vitreous plateau as described by Gray et al.²¹

CNVM Growth Inhibition

All experiments involving animal models were conducted with the approval of, and under compliance with standards set by, the local institutional animal care and use committee. Adult Brown Norway rats (Jackson Laboratories) were anesthetized via intraperitoneal injection of ketamine (0.1g/kg) and xylazine (0.01 g/kg) to induce sedation. Pupil dilation for rats was achieved by applying 1 drop per eye of a premixed suspension of 2.5% phenylephrine-HCl (Akron Pharmaceuticals) and 1% tropicamide (Akorn Pharmaceuticals). Using a technique published previously,²² Bruch's membrane was ruptured in each eye with thermal laser photocoagulation to induce CNVM growth. First, using a slit lamp laser delivery system, a glass coverslip was used to flatten the cornea and allow visualization of the optic nerve and retina. Next, 6 to 8 laser spots of 200 mW power, 50 μm diameter, and 100 ms duration were placed around the nerve, taking care to avoid retinal vessels. The goal was to create a visible bubble beneath the retina, indicating a rupture of Bruch's membrane. Spots that hemorrhaged or failed to create a bubble were excluded from the analysis.

Animals were assigned to 1 of 3 experimental groups: RO-101, aflibercept, or balanced saline solution (BSS). For each animal, 1 eye received 5 μl intravitreal injections of either RO-101 (6 mg/ml) or aflibercept (2 mg/0.05 ml) and the fellow eye served as the control, receiving an injection of 5 μl of BSS. The initial injection for each group was given immediately after laser photocoagulation. Intravitreal injections of 5 μl were delivered via a 32-gauge needle attached to a 10 μl syringe (Hamilton) using a method like that described by Gao et al.²³ Betadine solution (5%) was applied topically before any manipulation, and 0.3% ofloxacin ophthalmic solution was applied topically after each injection. Direct visualization with the slit lamp was used to confirm the proper placement of intravitreal injections. Animals with traumatic lens perforation were excluded from the study. Topical ofloxacin was applied daily for 1 week after treatment.

Two weeks post laser, animals were anesthetized, received intraperitoneal injection of fluorescein, and the eyes were harvested. Briefly, the left ventricle was cut, and a cannula was placed. A clamp was then used to occlude the descending aorta. The right atrium was also cut to allow for the outflow of perfusate. The vasculature was then perfused via the cannula with a constant flow pump (Harvard Apparatus). First, 120 ml of cold heparinized (1 IU/ml) PBS was infused. Then, 250 mg of 2×10^6 molecular-weight fluorescein isothiocyanate (FITC)—dextran (Sigma-Aldrich) in a volume of 50 ml of PBS was infused. Animals were euthanized with 100% CO_2 . Eyes were then enucleated and preserved in 10% formalin for 16 hours. The anterior portion and vitreous, and posterior portion of the eyes were dissected at the equator of the eye. Neural retina was then removed, and 4 radial cuts were made in the retinal pigment epithelium-choroid-sclera to flatten the tissue for flat mounting. Flat mounts were made from

these sections on standard microscope slides. The flat mounts were treated with an epifluorescent microscopy-specific medium (Bio-medex), and weights were placed on the coverslips for additional flattening.

Methods from Edelman and Castro were used to measure the FITC-dextran—labeled CNVM.²⁴ Flat mounts were examined with the 20x objective on an epifluorescent microscope and suitable FITC filters. Choroidal neovascularization was captured for analysis with a computer-operated digital camera. An observer, who was blinded to which eye received treatments, outlined the FITC-dextran perfused hyperfluorescent vessels using image capture and analysis software. To correct for the differing number of laser spots per eye, the total area of CNVM leakage was averaged for each treatment arm.

Human Umbilical Vein Endothelial Cells Migration Inhibition

Human umbilical vein endothelial cells (HUVECs) were purchased from ScienCell Research Laboratories and grown in a 5% CO_2 humidified incubator set at 37° C. Endothelial Cell Medium (ScienCell Research Laboratories) was used to allow for optimal proliferation. Culture inserts (Ibidi USA) were used to evaluate HUVEC migration potential. Thirty-five thousand HUVECs were seeded into a bifurcated chamber and placed in the incubator overnight. Eighteen hours after initial seeding, the culture inserts were removed, and cells were washed 3x with 1x PBS. After washing, media containing 40 ng of VEGF-A was added along with either bevacizumab, aflibercept, or surrobody (each at 2 nM concentration). Cells were incubated with the desired medium for 12 hours. The percent change in wound closure was calculated using an image of the same area over the 2 designated timepoints. This process was performed in triplicate and results were analyzed and reported.

Ocular Biocompatibility

All experiments involving animal models were conducted with the approval of, and under compliance with standards set by, the local institutional animal care and use committee.

Five Brown Norway rats received 5 μl intravitreal injections of either RO-101 (6 mg/ml) in the right eye or BSS in the left eye to evaluate for any ocular toxicity.

One month after injection, electroretinograms (ERGs) were performed. Animals were dark-adapted overnight before the ERG. Electroretinograms were performed on the Celeris device (Diagnosys LLC). The test consisted of flash stimuli at 0.01, 0.1, 1.0, and 3.0 $\text{cd} \cdot \text{s/m}^2$.

Post ERG testing, animals were sacrificed, and tissue was collected for histological analysis. The tissue was fixed, sectioned, and stained with hematoxylin and eosin. ImagePro (Media Cybernetics) software was used to quantify the number of cells present in the ganglion cell layer, inner nuclear cell layer, and outer nuclear cell layers. A program within ImagePro was written which looped through the following procedure: first, identify areas to quantify cells and place a preset perimeter around cells. Second, convert image to grayscale. Third, identify and quantify all cells. Analysis of each cell layer included the quantification of cells in 3 different areas of the layer.

VEGF-A and Ang-2 Target-Specific Binding Enzyme-Linked Immunosorbent Assay

VEGF-A specific (PeproTech, Cat #100-20) and Ang-2-specific (Acro Biosystems, Cat #AN2-H52H4) binding affinity of RO-101 was tested using enzyme-linked immunosorbent assay

(ELISA) on CHO cell derived materials (Lonza). Target coated plates were left overnight at room temperature, and the next day they were washed 3 times with PBS-0.05% Tween (PBST) and blocked with blocking buffer (PBST+1% BSA) for 1 hour at room temperature. The plates were washed again 3 times with PBST before adding a dilution series of RO-101 in blocking buffer and incubated for 1 hour at room temperature. The plates were then washed 3 times with PBST and then a 1:5000 dilution of Anti-Human IgG-horseradish peroxidase (HRP) antibody (Jackson ImmunoResearch, Cat. #709-035-098) was added and incubated for 1 hour at room temperature. The plates were then washed 6 times with PBST and then TMB substrate was added and incubated briefly at room temperature (typically 5 min). The stop solution was added and the plates read for absorbance at 450 nm. The binding affinity half maximal effective concentration (EC50) was determined using GraphPad Prism v 9 analysis.

Ligand-Receptor Competition ELISAs

To determine the inhibitory potencies of RO-101, we developed plate-based receptor ligand competition assays. To test competition between VEGF-A and its receptor VEGF R2/kinase insert domain receptor (KDR), we immobilized VEGF-A (Peprotech, Cat #100-20) and tested for binding against biotinylated recombinant human VEGF R2/KDR (rhVEGF R2/KDR, Acro Biosystems, Cat. KDR-H82E5) at a final 1 nM concentration. Test articles were added simultaneously to the addition of receptor and incubated for 1 hour at room temperature, followed by PBST washing. Next a 1:5000 dilution of HRP-conjugated streptavidin (Jackson ImmunoResearch Lab, Cat. #016-030-084) was added and incubated at room temperature for 1 hour and then followed by PBST washes. After the final wash, TMB substrate, stop, and colorimetric quantitation was repeated, similar to the target-binding ELISA section above. The half-maximal inhibitory concentration (IC50) values were determined using GraphPad Prism v 9 analysis.

To test Ang-2 competition, we used an assay similar to the VEGF receptor ligand competition, except that Tie2-Fc proteins (Acro Biosystems, Cat #T12-H5255) was coated and His-tagged Ang-2 (Acro Biosystems, Cat #AN2-H52H4) binding was detected by 1:10 000 dilution of HRP-conjugated anti-His antibody (Bethyl Laboratories, Cat. #A190-114P). All subsequent steps were similar to the VEGF receptor ligand and IC50 values were determined using GraphPad Prism v 9 analysis.

Statistical Analysis

All results are shown as means of measurements, taken in triplicate, followed by standard deviation of multiple measurements. Statistical analysis was performed using the Student paired *t* test and analysis of variance using statistical software (Excel, Microsoft Corporation) at the confidence level of 95%, with a *P* value of 0.05 considered statistically significant.

Results

The surrobody platform is an approach to both enhance and simplify antibody discovery and design that was first described in relation to antiviral antibodies discovered from H5N1 avian flu survivors.²⁵ The surrobody structure is similar to a traditional antibody (Fig 1) but instead of using canonical light chains, HC complementation is accomplished with an invariant SLC. The invariant SLC provides the potential to rapidly create bispecific therapeutics in an accelerated and robust manner with

simplified “plug and play” characteristics that avoid complex protein engineering, especially that associated with light-chain mismatching.^{25–27}

Vitreous Half-Life

To determine intraocular half-life, we injected fluorescently labeled RO-101 into the vitreous of New Zealand White Cross rabbits. Calculations based upon fluorescent measurements taken from peak average measurements support a vitreous half-life estimate of 6.75 days \pm 2.13 days (Table 1)^{28–32} that compares favorably to previously published rabbit vitreous half-life assessments.

CNVM Inhibition

RO-101 demonstrated efficacy by decreasing the total amount of CNVM leakage after laser photocoagulation insult. The mean CNVM leakage area in vehicle-treated eyes was 3066 \pm 839 K pixels whereas eyes treated with RO-101 reduced the leakage area by 59% (1259 \pm 106 K pixels). The RO-101 reduction compared favorably to aflibercept-treated eyes that reduced leakage area by 53%. Two-way analysis of variance comparing BSS and RO-101 as well as BSS and aflibercept were statistically significant (*P* value = 0.0015) (Fig 2).

HUVEC Migration Inhibition

We used a VEGF-induced HUVEC migration as a comparative bioassay. We found at 12 hours, HUVEC cells exposed to both 40 ng of VEGF-A and aflibercept demonstrated a 70% reduction in VEGF-induced migration, compared with control cells exposed to VEGF-A alone. Human umbilical vein endothelial cells exposed to 40 ng of VEGF-A and bevacizumab yielded only a 22% reduction, and by further comparison, cells exposed to 40 ng of VEGF-A and RO-101 resulted in a 68% reduction in VEGF-induced migration compared with control. Using 2-sample *t* tests, the difference in reduction in VEGF-induced HUVEC migration between aflibercept and RO-101 was not significant (*P* = 0.93), but was significant between RO-101 and bevacizumab (*P* = 0.003) and between RO-101 and VEGF-A alone (*P* = 0.002) (Fig 3A). A single factor analysis of variance yielded a *P* value of 7.37×10^{-5} , indicating a difference in the average migration between the 4 groups.

Ocular Biocompatibility

As a safety surrogate assessment, we tested ocular tolerability by both histological and real-time ERG readings in Brown Norway rats. Histological analysis between RO-101 and BSS showed no statistically significant difference in cell count between ganglion cells (17.90 \pm 1.31, *R* = 16.33 \pm 1.11, *t* test = 0.40), outer nuclear layers (156.04 \pm 2.49, *R* = 153.09 \pm 3.19, *t* test = 0.42), or inner nuclear layers (56.33 \pm 2.11, *R* = 56.38 \pm 1.42, *t* test = 0.98) of the retina (Fig 4). Electroretinogram analysis of scotopic and photopic light response showed cone and rod functional activity with no statistically significant difference in the A and B wave amplitudes and peak times between the control and the experimental eye. Figure 5 is an illustration of a similar

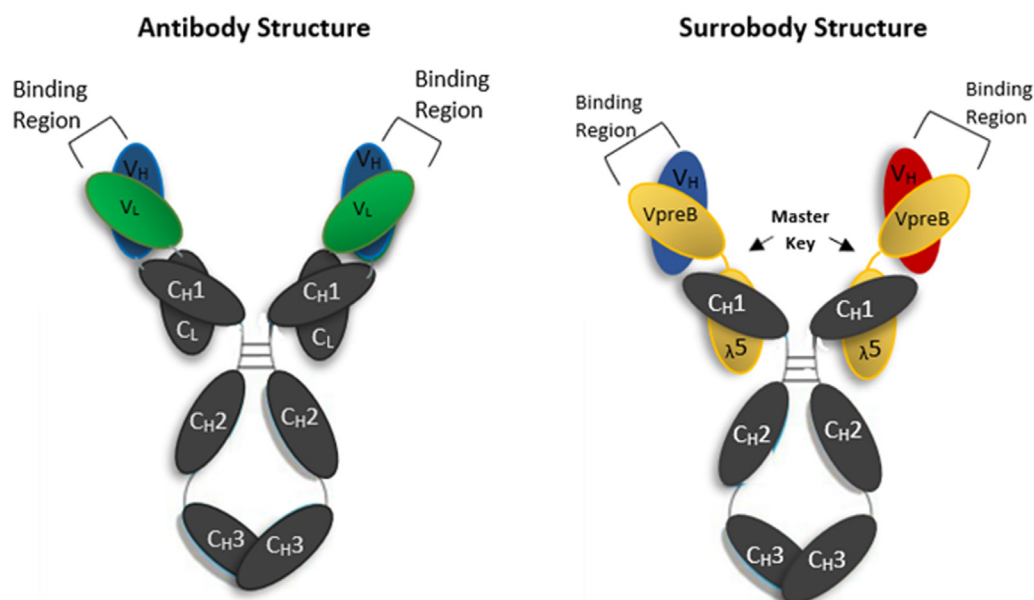


Figure 1. The typical monoclonal antibody has a variable light chain (VL, green) that is unique and required for specific target binding. The Surrobody structure uses an invariant surrogate light chain (yellow), providing a universal partner to all heavy chain partners in the Surrobody library to streamline drug discovery and manufacturing.

ERG response in the experiment and control arm at flash stimuli of 3.0 cd·s/m². Electroretinogram readings from the eyes exposed to RO-101 and BSS showed no difference in the amplitude and response times between experimental and control eyes.

VEGF-A and Ang-2 Target-Specific Binding and Inhibition of Target-Receptor Interaction as Determined by ELISA

RO-101 was tested in a target-specific ELISA assay alongside aflibercept and faricimab for reference as current clinical therapeutics, and trastuzumab for a nonbinding, nonspecific control. RO-101's binding affinity for VEGF-A demonstrated EC50 of 0.040 nM. Three lines of RO-101 were tested with similar results (results not shown). This was shown to be comparable to aflibercept and faricimab (Fig 6).

Binding affinity to Ang-2 was also tested using ELISA assay alongside aflibercept, faricimab, and trastuzumab in a similar fashion. RO-101's binding affinity was robust, with an EC50 of 0.054 nM. Faricimab showed a significantly lower binding affinity and as expected, no Ang-2 binding was identified for aflibercept (Fig 7).

To examine how potently RO-101 blocks target-receptor interaction, the inhibition of target-receptor binding in

ELISA was performed and compared with faricimab. For VEGF-A and its receptor VEGF R2/KDR binding, the VEGF-A was captured on plate wells and the binding of biotinylated VEGF R2/KDR was competed with serial diluted RO-101 or faricimab. The remaining binding of VEGF R2/KDR was detected by HRP-conjugated streptavidin. In this format, RO-101 was able to inhibit the binding at an IC50 of 1.989 nM, whereas faricimab inhibited the binding at an IC50 of 6.471 nM, a threefold weaker inhibition than RO-101 (Fig 8).

Inhibition of Ang-2 and its receptor Tie-2 binding was tested in a similar fashion. The plate well-captured Tie-2 had competition for Ang-2 binding by RO-101 or faricimab. RO-101 was able to inhibit the binding at an IC50 of 0.7868 nM. faricimab inhibited the binding at an IC50 of 13.55 nM, showing 17-fold weaker inhibition than RO-101 (Fig 9).

Discussion

Current anti-VEGF-A monotherapy has made significant inroads in treating eAMD. However, despite treatment, 45% of patients in studies have been termed “non-responders” or poor responders who show a suboptimal response to therapy, with recalcitrant fluid or the inability to extend to

Table 1. Rabbit Vitreous Half-Life of RO-101 Compared with Similar Previously Published Preclinical Data

Rabbit Vitreous Study	RO-101 (Current Study)	Aflibercept	Bevacizumab	Faricimab	Ranibizumab
Half-life (days)	6.75 ± 2.13	3.92-4.58 ^{28,32}	4.32-6.61 ^{29,32}	4.29 ³⁰	2.75-2.9 ^{29,31,32}

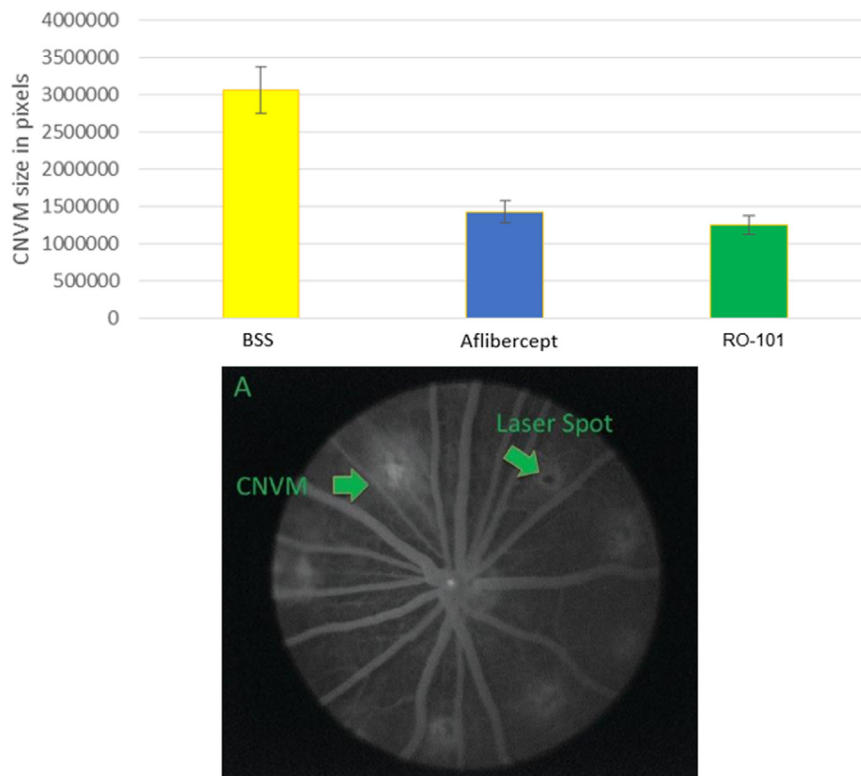


Figure 2. Choroidal neovascular membrane (CNVM) size in pixels post injection of therapeutic agent was similar among RO-101 and aflibercept whereas both were shown to be superior to control (balanced saline solution, BSS) at preventing choroidal neovascularization (P value = 0.0015) using 2-way analysis of variance. There was no statistically significant difference between aflibercept and RO-101.

labeled dosing schedules.^{15–19} Furthermore, the high injection burden in these nonresponders may lead to poor patient compliance and worse visual outcomes.³³ The Comparison of AMD Treatment Trials is evidence that visit adherence contributes to better visual outcomes.³⁴ The Comparison of AMD Treatment Trials also displayed a regression of visual acuity gains in the 5-year follow-up data, largely presumed to be a function of decreasing compliance with study protocol after leaving the active portion of the study. Therefore, it is important to strive for therapies that reduce treatment burden without compromising visual acuity.³⁵ It could be postulated that a therapeutic agent targeting multiple soluble factors necessary for angiogenesis, such as VEGF-A and Ang-2, could potentially better treat this subset of nonresponders than current anti-VEGF-A monotherapies. Given the rapid clinical adoption of faricimab, and data that have been presented in the Truckee trial, it is evident that there is potential merit to this argument in the clinical setting.³⁶

Above all else, a therapeutic must demonstrate ocular compatibility in animals, as well as efficacy, to be able to advance to be an intravitreal therapeutic agent. With the postmarket authorization experience of brolicuzumab and the more recent experience with pegcetacoplan, immunologic tolerance must be established at every stage of the process from preclinical data to postmarketing surveillance.

RO-101 demonstrates ocular tolerability in rabbit models and revealed no signs of inflammation in both rabbit and rat models throughout all the experiments described in this paper. In addition, RO-101 demonstrated efficacy in a rat laser CNVM model on par with aflibercept in terms of efficacy. Both characteristics support RO-101 advancing to further preclinical testing.

In addition to therapies with multiple targets, therapies with increased biological activity can potentially reduce the frequency of patient visits as well as the injection burden. There are 3 pharmacologic strategies to achieve greater biological activity and extend disease remission: increase molar dose, increase half-life, and increase binding affinity (Fig 10). Increasing molar dosage, the concentration of particles in a solution administered at a single time to the patient,³⁷ has been a common strategy to increase biologic activity since the results of the pivotal HARBOR trial. The HARBOR trial was used to evaluate the safety and efficacy of ranibizumab at 0.5 mg versus 2.0 mg over 12 months and 24 months, both monthly and pro re nata.³⁸ In the pro re nata arm of the study, the average interval between doses, after the loading phase of 3 monthly injections, was longer in patients who received 2.0 mg (12.5 vs. 9.9 weeks). This suggests that administering a higher dose of intravitreal ranibizumab could result in longer biological activity of the agent. As-needed dosing

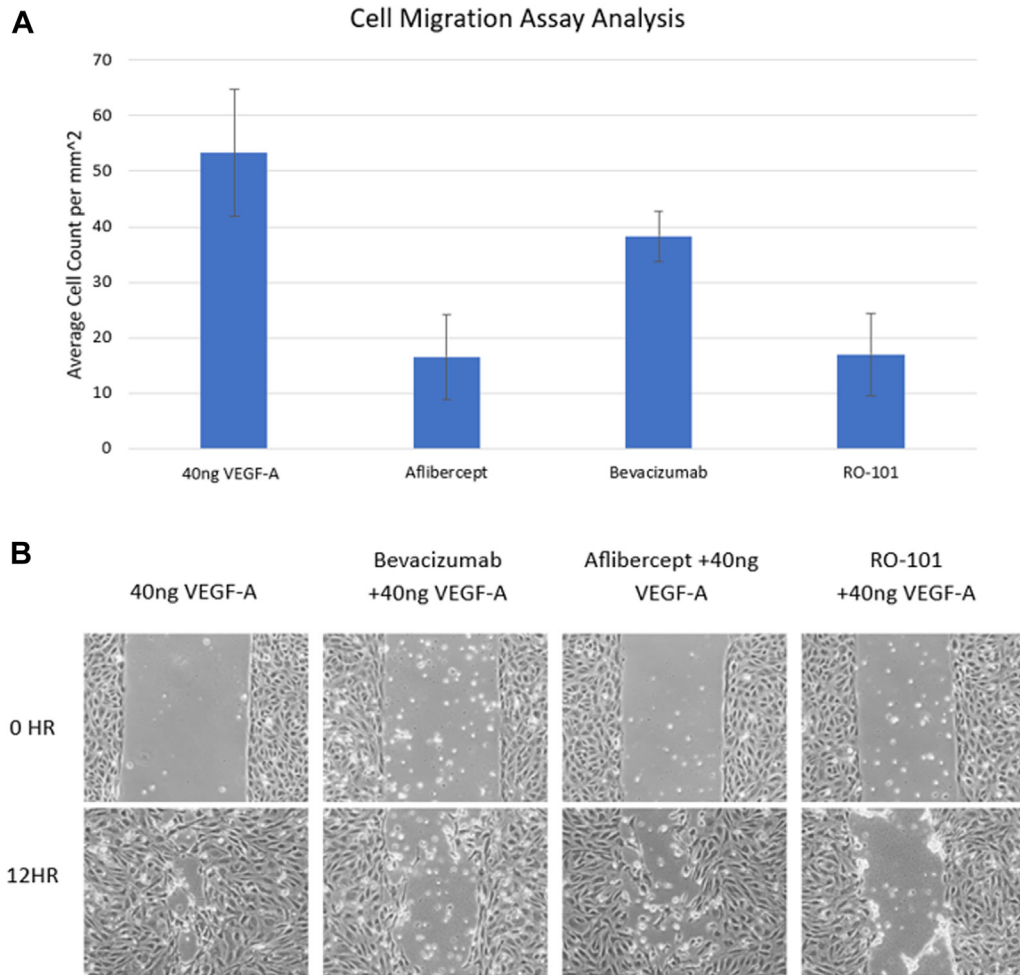


Figure 3. Human umbilical vein endothelial cell (HUVEC) wound closure analysis. Quantitative analysis of VEGF-A induced cell migration and effects of aflibercept, bevacizumab, or RO-101 treatment **A**, Representative images of wound closure of HUVECs after exposure to VEGF-A and either bevacizumab, aflibercept, or RO-101 at 0 and 12 hours **B**, Replicate analysis of images at 0 hours were deemed to be comparable.

with 2.0 mg also showed a significant decrease in central foveal thickness (−181.0 vs. −171.8 micrometers) as compared with 0.5 mg, which could be an effect of increased duration of biologic activity of the therapeutic.³² The molar dose of RO-101 can be modeled off well-established therapeutics to get an effect of the same or increased caliber.

A greater half-life allows a longer duration of biological activity in the vitreous of the eye. Thus, increasing half-life results in increased intervals between necessary treatments, decreasing the treatment burden with any given agent. RO-101 shows superior half-life attributes (6.75 ± 2.13 days) in the vitreous compared with previously published data for aflibercept (3.92 days),²⁸ ranibizumab (Lucentis, Genentech/Roche; 2.88 days),²⁹ faricimab (4.29 days),³⁰ and bevacizumab (Avastin, Genentech/Roche; 6.51 days).^{31,32} This gives RO-101 the potential for a longer duration of biological activity, reducing the

frequency of injections and treatment burden for patients suffering from eAMD.

A higher affinity can potentially lower the minimal efficacious concentration required to block a given factor. RO-101's binding affinity for VEGF-A is similar to other therapies in the market (aflibercept and faricimab), with an EC50 of 0.040 nM. However, RO-101 has a superior binding affinity for Ang-2 (EC50 0.05 nM) compared with faricimab (EC50 3.5 nM), the only approved bispecific that targets Ang-2. With an EC50 that is 70 times greater than faricimab, RO-101 should demonstrate biological activity against Ang-2 at much lower concentrations, potentially extending durability.

Ultimately, a therapeutic agent's binding affinity is an indirect measurement of its ability to inhibit a given target-receptor interaction. VEGF and Ang-2, when binding to their receptors and acting together, promote neovascularization. Decreasing the interaction of VEGF-A and

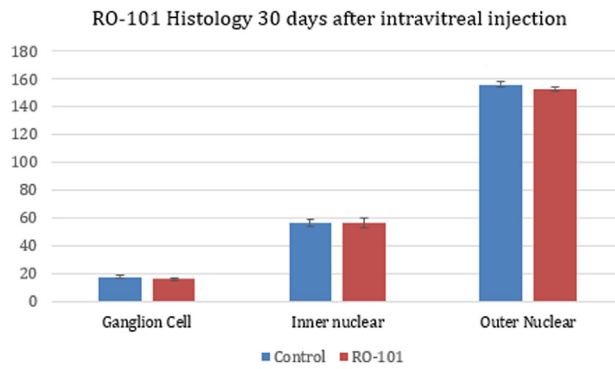
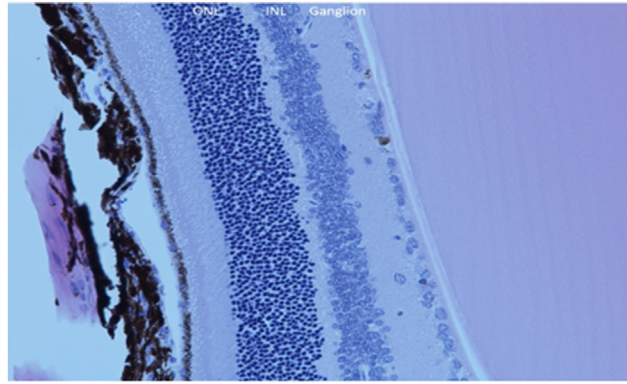


Figure 4. Average cell counts in the ganglion cell layer, inner nuclear cells layer (INL), and outer nuclear cell layer (ONL) of the retina in Brown Norway rats after control or RO-101 treatment.

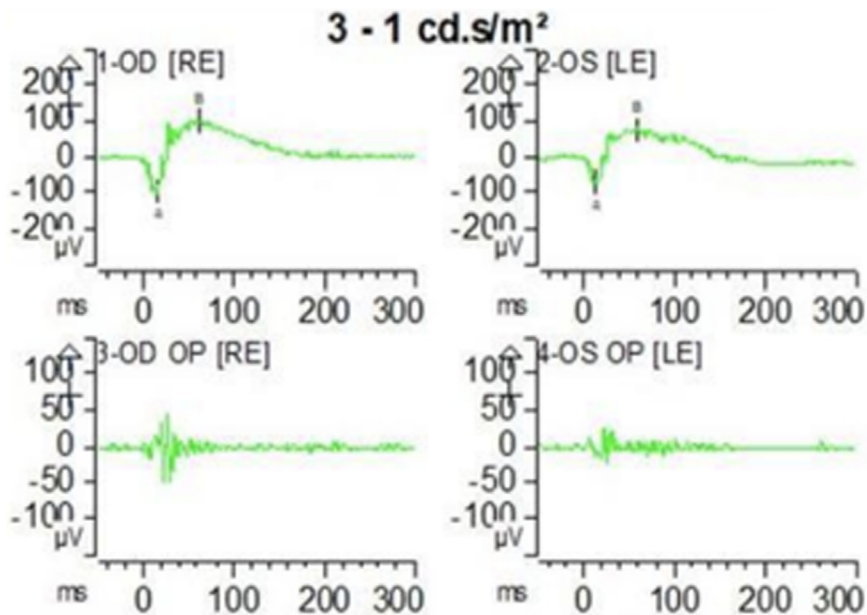


Figure 5. Electroretinogram readings were taken after exposure to RO-101 in the right eye (OD) and balanced saline solution (BSS) as the control in the left eye (OS). The left image shows the amplitude and response times of the experimental eye. The right images show the amplitude and response times of the control eye with BSS.

Trastuzumab	Faricimab	Aflibercept	RO-101
No binding	41.61pM	51.35pM	40.15pM

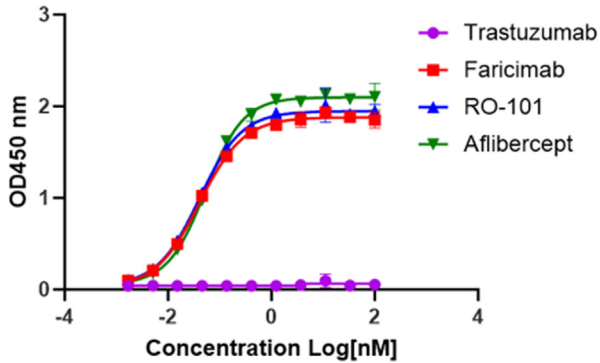


Figure 6. Binding affinities to VEGF as demonstrated by half maximal effective concentration of RO-101, aflibercept, faricimab, and negative control trastuzumab are shown.

Ang-2 with their receptors can decrease the potential for either to have this effect.³⁹ RO-101 demonstrated IC50 toward VEGF-A target-receptor interaction at 1.989 nM, which is about threefold better than faricimab's IC50 at 6.471. RO-101 was also superior at preventing Ang-2 target-receptor interaction with an IC50 of 0.7868 nM, nearly 17-fold better compared with faricimab with an IC50 of 13.55 nM. This difference in target-receptor inhibition of VEGF-A and Ang-2 compared with faricimab may confer

Trastuzumab	Faricimab	Aflibercept	RO-101
No binding	3508pM	No binding	53.58pM

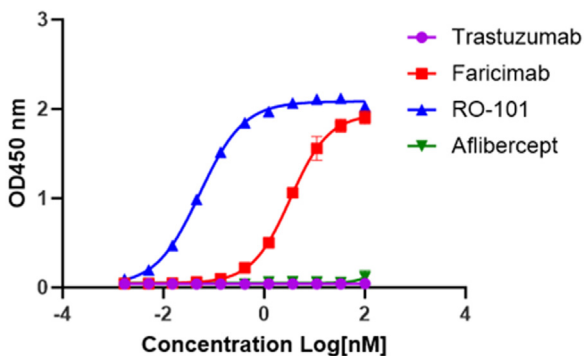


Figure 7. Binding affinities to angiopoietin-2 as demonstrated by half maximal effective concentration of RO-101, aflibercept, faricimab, and negative control trastuzumab.

Control	Faricimab (Vabysmo) IC50	RO-101 IC50	RO-101 and Faricimab Comparison
No binding inhibition	6.471 nM	1.989 nM	3.25x

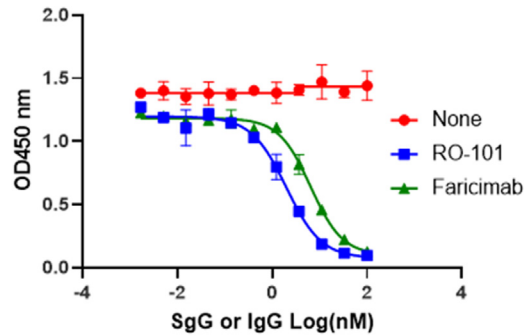


Figure 8. The inhibition of VEGF-A and VEGF R2/kinase insert domain receptor (receptor of VEGF-A) binding in enzyme-linked immunosorbent assay; is shown. IC50 = half-maximal inhibitory concentration.

an advantage in the duration of efficacy by effectively target binding at lower concentrations compared with faricimab.

RO-101 has been demonstrated to be similar or superior to current intravitreal therapies for the treatment of eAMD with regard to molar dose, affinity, and half-life. These findings support the possibility that RO-101 will have a beneficial clinical impact in achieving disease remission in the subset of patients who show suboptimal or no improvement with currently available treatment options. These preclinical data are supportive of the need for further research and preclinical development with RO-101.

Control	Faricimab IC50	RO-101 IC50	RO-101 improvement over Faricimab
No binding inhibition	13.55nM	0.7868nM	17.2x

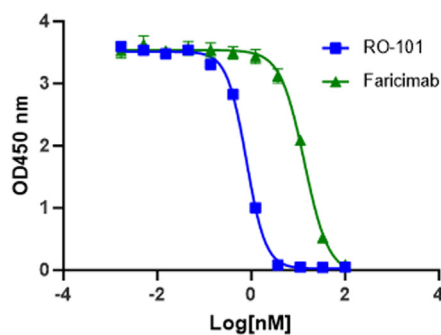


Figure 9. The inhibition of angiopoietin-2 (Ang-2) and Tie-2 (receptor of Ang-2) binding in enzyme-linked immunosorbent assay is shown. IC50 = half-maximal inhibitory concentration.

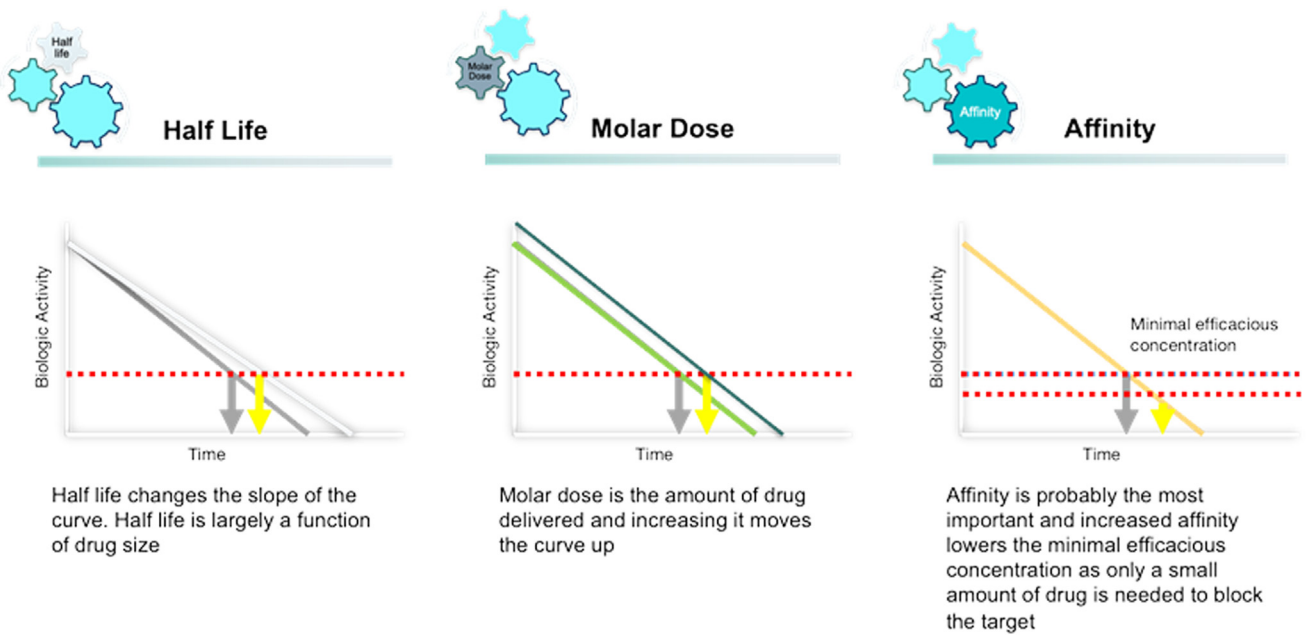


Figure 10. Three different strategies to extend disease remission are to increase the molar dose, affinity, and half-life.

Footnotes and Disclosures

Originally received: September 12, 2023.

Final revision: December 18, 2023.

Accepted: January 11, 2024.

Available online: January 18, 2024. Manuscript no. XOPS-D-23-00225R1.

¹ Independent Research Consultant, Contrator for RevOpsis Therapeutics, Inc., San Carlos, California.

² Springfield Clinic Eye Institute, Springfield, Illinois.

³ Retina Department. Asociacion para Evitar la Ceguera en Mexico IAP, Mexico City, Mexico.

⁴ University of Missouri-Kansas City School of Medicine, Kansas City, Missouri.

⁵ Retinal Consultants of Arizona, and University of Arizona College of Medicine, Phoenix, Arizona.

⁶ Vanderbilt School of Medicine, Nashville, Tennessee.

⁷ Sierra Eye Associates, and University of Nevada, Reno School of Medicine, Reno, Nevada.

⁸ Cole Eye Institute, Cleveland, Ohio.

⁹ Ophthalmic Consultants of Boston, Boston, Massachusetts.

¹⁰ Sue Anschutz Rodgers Eye Center, University of Colorado, Aurora, Colorado.

¹¹ University of Michigan Kellogg Eye Center, Ann Arbor, Michigan.

Disclosure(s):

All authors have completed and submitted the ICMJE disclosures form.

The author(s) have made the following disclosure(s): L.X.: Support – RevOpsis Therapeutics; Consulting fees – RevOpsis Therapeutics; Speaker fees – RevOpsis Therapeutics; Patents planned, issued or pending – RevOpsis Therapeutics; Stock options – RevOpsis Therapeutics.

J.R.P.: Support – RevOpsis Therapeutics; Stock options – RevOpsis Therapeutics; Other services – Genentech, Apellis, Horizon.

M.R.B.: Support – RevOpsis Therapeutics; Grants or contracts – Adverum Biotech, Annexon Biosciences, CalciMedica, Clearside Biomedical, Eye-Point Pharma, Gemini Therapeutics, Genentech, Gyroscope Therapeutics, Kodiak Sciences, Novartis, Ocular Therapeutix, Oculis, Opthea, Oxular,

Oxurion, RegenxBio, ReNeuron, Ribomic, Roche, Stealth Biotherapeutics, Unity Biotechnology; Consulting fees – AbbVie Inc., Adverum Biotech, Alcon, Alimera, Allegro, Allergan, AmerisourceBergen, Annexon, Apellis, Arctic Vision, Bausch and Lomb, Biogen, CalciMedica, Clearside, Biomedical, Coherus Biosciences, EyePoint Pharma, Genentech, Kodiak Sciences, Iveric Bio, Neurotech, Novartis, Ocular Therapeutix, Opthea, Outlook Therapeutics, Palatin Technologies, Regeneron, RegenxBio, RevOpsis Therapeutics, Roche, Stealth Biotherapeutics; Speaker fees – Apellis, Iveric Bio, Bausch and Lomb, Novartis, Genentech, Regeneron; Participation on a Data Safety Monitoring Board or Advisory Board – Clearside Biomedical; Stock options – NeuBase, Oxurion, RevOpsis Therapeutics.

R.L.: Support – RevOpsis Therapeutics; Stock options – RevOpsis Therapeutics.

A.M.K.: Support – RevOpsis Therapeutics.

P.K.K.: Consulting fees – AffaMed Therapeutics, Alcon, Allegro, Allergan, Allgenesis, Alynlyam Pharmaceuticals, Alzheon, Annexon Biosciences, AsclepiX, Aviceda, Bayer, Bausch and Lomb, Beacon Therapeutics (AGTC), Biogen Idec, Bionic Vision Technologies, Boehringer Ingelheim, Clearside Biomedical, Coherus, Complement Therapeutics, DelSiTech, Dompe, Duet Therapeutics, Eyeevensys, Galecto Biotech, Galimedix, Genentech/Roche, Glaukos, Innovent, InterGalactic Therapeutics, iRenix, jCyte, Kanaph Therapeutics, Kanghong, Kera Therapeutics, Kodiak, Kriya Therapeutics, Nanoscope Therapeutics, Novartis, Ocugenix, Ocular Therapeutix, Oculis, Ocuphire, OcuTerra Therapeutics, Omeros, Oxurion, Palatin, Regeneron, RegenxBio, Resonance Medicine Inc., RetinaAI Medical AG, Retinal Sciences, ReVana, Roivant, Samsung Bioepis, SGN Nanopharma Inc., Stealth Biotherapeutics, Stuart, Sustained Nano Systems, Takeda, Théa, Unity Biotechnology, VisgenX, 2020 Onsite, 4D Molecular Therapeutics; Stock options – Ocular Therapeutix; Other services – Carl Zeiss Meditec.

J.S.H.: Grants or contracts – 4D Molecular Technologies, Annexon, Apellis, AsclepiX Therapeutics, Ashvattha, Bayer, Cognition Therapeutics, Curacle, Genentech/Roche, Gyroscope Therapeutics, Iveric Bio, Janssen R&D, Kodiak, NGM, Novartis, OcuTerra, Perceive Bio, Regeneron

Pharmaceuticals, Inc., REGENXBIO; Consulting fees — 4D Molecular Therapeutics, Abpro, Adverum, AffaMed Therapeutics, Applied Genetics Technologies Corporation, Akouos, Annexon, Apellis, AsclepiX Therapeutics, Aviceda, Bausch + Lomb, Biovisics, Clearside, Curacle, DTx Pharma, Exegensis, Genentech/Roche, Glaukos, Gyroscope Therapeutics, Immunogen, Iveric Bio, Janssen R&D, jCyte, Kriya, Nanoscope, NGM, Notal Vision, Novartis, Ocular Therapeutix, Ocuphire, OcuTerra, OliX, ONL Therapeutics, Outlook Therapeutics, Palatin Technologies, Perceive Biotherapeutics, Ray Therapeutics, Regeneron Pharmaceuticals, Inc., REGENXBIO, RetinAI, RevOpsis Therapeutics, Stealth BioTherapeutics, Théa Pharmaceuticals, Vanotech; Leadership or fiduciary role — ASRS, Retina Society, Ocular Therapeutics; Stock options — Adverum, Aldeyra, Allegro, Aviceda, jCyte, Ocuphire, Ocular Therapeutix, RevOpsis Therapeutics, Vinci, Vitranu.

J.L.O.: Support — RevOpsis Therapeutics

R. Bhat: Support — RevOpsis Therapeutics; Consulting fees — RevOpsis Therapeutics; Patents planned, issued or pending — RevOpsis Therapeutics; Stock options — RevOpsis Therapeutics.

R. Bhandari: Support — RevOpsis Therapeutics; Consulting fees — Apellis, Novartis, Regeneron, RegenXBio; Speaker fees — Regeneron, RegenXBio; Travel support — Regeneron, RegenXBio; Patents planned, issued or pending — RevOpsis Therapeutics, Inc., University of CO; Leadership or fiduciary role in other board — Springfield Clinic, RevOpsis Therapeutics; Stock options — RevOpsis Therapeutics, Eli Lilly, Talaris Therapeutics; Other services — Genentech, Apellis, Bausch & Lomb, Horizon, Regeneron, Novartis, EyePoint Pharmaceuticals.

The other authors have no proprietary or commercial interest in any materials discussed in this article.

HUMAN SUBJECTS: No human subjects were included in this study.

Animal subjects were included in this study. All experiments involving animal models were conducted with approval of, and under compliance of standards set by, the local institutional animal care and use committee.

Author Contributions:

Conception and design: Xu, Jones, Morgenstern, Caldwell, Mueller, Quiroz-Mercado, Huvard, Olson

Data collection: Xu, Prentice, Gupta, Jones, Morgenstern, Caldwell, Mueller, Quiroz-Mercado, Huvard, Olson

Analysis and interpretation: Xu, Prentice, Sinha, Gupta, Khanani, Kaiser, Heier, Olson, Bhatt, Bhandari

Obtained funding: Study was performed as part of regular employment duties at RevOpsis Therapeutics, Inc. No additional funding was provided.

Overall responsibility: Bhandari

Abbreviations and Acronyms:

Ang-2 = angiotensin-2; **BSS** = balanced saline solution; **CNVM** = choroidal neovascular membrane; **eAMD** = exudative age-related macular degeneration; **EC50** = half maximal effective concentration; **ELISA** = enzyme-linked immunosorbent assay; **ERG** = electroretinograms; **FITC** = fluorescein isothiocyanate; **HC** = heavy chain; **HRP** = horseradish peroxidase; **HUVEC** = human umbilical vein endothelial cell; **IC50** = half-maximal inhibitory concentration; **KDR** = kinase insert domain receptor; **PBS** = phosphate balanced saline; **PBST** = phosphate balanced saline-0.05% Tween; **SLC** = surrogate light chain.

Keywords:

AMD, Ang-2, Anti-VEGF, Bispecific, Surrobody.

Correspondence:

Ramanath Bhandari, MD, 1025 S 6th Street, Springfield, IL 62711. E-mail: ramanath.bhandari@gmail.com.

References

- Campochiaro PA. Ocular neovascularization. *J Mol Med (Berl)*. 2013;91:311–321. <https://doi.org/10.1007/s00109-013-0993-5>.
- Kvanta A, Alverve PV, Berglin L, Seregard S. Subfoveal fibrovascular membranes in age-related macular degeneration express vascular endothelial growth factor. *Invest Ophthalmol Vis Sci*. 1996;37:1929–1934.
- Lopez PF, Sippy BD, Lambert HM, Thach AB, Hinton DR. Transdifferentiated retinal pigment epithelial cells are immunoreactive for vascular endothelial growth factor in surgically excised age-related macular degeneration-related choroidal neovascular membranes. *Invest Ophthalmol Vis Sci*. 1996;37:855–868.
- Adamis AP, Miller JW, Bernal MT, et al. Increased vascular endothelial growth factor levels in the vitreous of eyes with proliferative diabetic retinopathy. *Am J Ophthalmol*. 1994;118:445–450. [https://doi.org/10.1016/s0002-9394\(14\)75794-0](https://doi.org/10.1016/s0002-9394(14)75794-0).
- Aiello LP, Avery RL, Arrigg PG, et al. Vascular endothelial growth factor in ocular fluid of patients with diabetic retinopathy and other retinal disorders. *N Engl J Med*. 1994;331:1480–1487. <https://doi.org/10.1056/NEJM199412013312203>.
- Krzystolik MG, Afshari MA, Adamis AP, et al. Prevention of experimental choroidal neovascularization with intravitreal anti-vascular endothelial growth factor antibody fragment. *Arch Ophthalmol*. 2002;120:338–346. <https://doi.org/10.1001/archophth.120.3.338>.
- Pe'er J, Shweiki D, Itin A, Hemo I, Gnessin H, Keshet E. Hypoxia-induced expression of vascular endothelial growth factor by retinal cells is a common factor in neovascularizing ocular diseases. *Lab Invest*. 1995;72:638–645.
- Malecize F, Clamens S, Simorre-Pinatel V, et al. Detection of vascular endothelial growth factor messenger RNA and vascular endothelial growth factor-like activity in proliferative diabetic retinopathy. *Arch Ophthalmol*. 1994;112:1476–1482. <https://doi.org/10.1001/archophth.1994.01090230090028>.
- Jo N, Mailhos C, Ju M, et al. Inhibition of platelet-derived growth factor B signaling enhances the efficacy of anti-vascular endothelial growth factor therapy in multiple models of ocular neovascularization. *Am J Pathol*. 2006;168:2036–2053. <https://doi.org/10.2353/ajpath.2006.050588>.
- Ziegler T, Horstkotte J, Schwab C, et al. Angiotensin 2 mediates microvascular and hemodynamic alterations in sepsis. *J Clin Invest*. 2013;123:3436–3445. <https://doi.org/10.1172/JCI66549>.
- Oshima Y, Deering T, Oshima S, et al. Angiotensin-2 enhances retinal vessel sensitivity to vascular endothelial growth factor. *J Cell Physiol*. 2004;199:412–417. <https://doi.org/10.1002/jcp.10442>.
- Oshima Y, Oshima S, Nambu H, et al. Different effects of angiotensin-2 in different vascular beds: new vessels are most sensitive. *FASEB J*. 2005;19:963–965. <https://doi.org/10.1096/fj.04-2209fje>.
- Watanabe D, Suzuma K, Suzuma I, et al. Vitreous levels of angiotensin 2 and vascular endothelial growth factor in patients with proliferative diabetic retinopathy. *Am J Ophthalmol*. 2005;139:476–481. <https://doi.org/10.1016/j.ajo.2004.10.004>.

14. Loukovaara S, Robciuc A, Holopainen JM, et al. Ang-2 upregulation correlates with increased levels of MMP-9, VEGF, EPO and TGFβ1 in diabetic eyes undergoing vitrectomy. *Acta Ophthalmol.* 2013;91:531–539. <https://doi.org/10.1111/j.1755-3768.2012.02473.x>.
15. Rosenfeld PJ, Brown DM, Heier JS, et al. Ranibizumab for neovascular age-related macular degeneration. *N Engl J Med.* 2006;355:1419–1431. <https://doi.org/10.1056/NEJMoa054481>.
16. Rosenfeld PJ, Rich RM, Lalwani GA. Ranibizumab: phase III clinical trial results. *Ophthalmol Clin North Am.* 2006;19:361–372. <https://doi.org/10.1016/j.ohc.2006.05.009>.
17. Chang TS, Bressler NM, Fine JT, et al. Improved vision-related function after ranibizumab treatment of neovascular age-related macular degeneration: results of a randomized clinical trial. *Arch Ophthalmol.* 2007;125:1460–1469. <https://doi.org/10.1001/archophth.125.11.1460>.
18. Brown DM, Michels M, Kaiser PK, et al. Ranibizumab versus verteporfin photodynamic therapy for neovascular age-related macular degeneration: two-year results of the Anchor study. *Ophthalmology.* 2009;116:57–65.e5. <https://doi.org/10.1016/j.ophtha.2008.10.018>.
19. Lux A, Llacer H, Heussen FM, Jousseaume AM. Non-responders to bevacizumab (Avastin) therapy of choroidal neovascular lesions. *Br J Ophthalmol.* 2007;91:1318–1322. <https://doi.org/10.1136/bjo.2006.113902>.
20. Brown DM, Boyer DS, Csaky K, et al. Intravitreal nesvacumab (antiangiopoietin 2) plus aflibercept in diabetic macular edema: phase 2 RUBY randomized trial. *Retina.* 2022;42:1111–1120. <https://doi.org/10.1097/IAE.0000000000003441>.
21. Gray JR, Mosier MA, Ishimoto BM. Optimized protocol for Fluorotron Master. *Graefes Arch Clin Exp Ophthalmol.* 1985;22:225–229. <https://doi.org/10.1007/BF02133684>.
22. Olson JL, Courtney RJ, Rouhani B, Mandava N, Dinarello CA. Intravitreal anakinra inhibits choroidal neovascular membrane growth in a rat model. *Ocul Immunol Inflamm.* 2009;17:195–200. <https://doi.org/10.1080/09273940802710705>.
23. Gao H, Qiao X, Gao R, Mieler WF, McPherson AR, Holz ER. Intravitreal triamcinolone does not alter basal vascular endothelial growth factor mRNA expression in rat retina. *Vision Res.* 2004;44:349–356. <https://doi.org/10.1016/j.visres.2003.09.027>.
24. Edelman JL, Castro MR. Quantitative image analysis of laser-induced choroidal neovascularization in rat. *Exp Eye Res.* 2000;71:523–533. <https://doi.org/10.1006/exer.2000.0907>.
25. Xu L, Yee H, Chan C, et al. Combinatorial Surrobody libraries. *Proc Natl Acad Sci U S A.* 2008;105:10756–10761. <https://doi.org/10.1073/pnas.0805293105>.
26. Huse WD, Sastry L, Iverson SA, et al. Generation of a large combinatorial library of the immunoglobulin repertoire in phage lambda. *Science.* 1989;246:1275–1281. <https://doi.org/10.1126/science.2531466>.
27. Lerner RA. Manufacturing immunity to disease in a test tube: the magic bullet realized. *Angew Chem Int Ed Engl.* 2006;45:8106–8125. <https://doi.org/10.1002/anie.200603381>.
28. Park SJ, Choi Y, Na YM, et al. Intraocular pharmacokinetics of intravitreal aflibercept (Eylea) in a rabbit model. *Invest Ophthalmol Vis Sci.* 2016;57:2612–2617. <https://doi.org/10.1167/iovs.16-19204>.
29. Bakri SJ, Snyder MR, Reid JM, Pulido JS, Ezzat MK, Singh RJ. Pharmacokinetics of intravitreal ranibizumab (Lucentis). *Ophthalmology.* 2007;114:2179–2182. <https://doi.org/10.1016/j.ophtha.2007.09.012>.
30. United States Food and Drug Administration/Center for Drug Evaluation and Research. *Nonclinical Review(s)*. Application number 761235Orig1s000. 2021. Genentech, Inc. https://www.accessdata.fda.gov/drugsatfda_docs/nda/2022/761235Orig1s000/PharmR.pdf. Accessed April 1, 2023.
31. Sinapis CI, Routsias JG, Sinapis AI, et al. Pharmacokinetics of intravitreal bevacizumab (Avastin®) in rabbits. *Clin Ophthalmol.* 2011;5:697–704. <https://doi.org/10.2147/OPTH.S19555>.
32. García-Quintanilla L, Luaces-Rodríguez A, Gil-Martínez M, et al. Pharmacokinetics of intravitreal anti-VEGF drugs in age-related macular degeneration. *Pharmaceutics.* 2019;11:365. <https://doi.org/10.3390/pharmaceutics11080365>.
33. Polat O, İnan S, Özcan S, et al. Factors affecting compliance to intravitreal anti-vascular endothelial growth factor therapy in patients with age-related macular degeneration. *Turk J Ophthalmol.* 2017;47:205–210. <https://doi.org/10.4274/tjo.28003>.
34. Comparison of Age-related Macular Degeneration Treatments Trials (CATT) Research Group, Maguire MG, Martin DF, et al. Five-year outcomes with anti-vascular endothelial growth factor treatment of neovascular age-related macular degeneration: the comparison of age-related macular degeneration treatments trials. *Ophthalmology.* 2016;123:1751–1761. <https://doi.org/10.1016/j.ophtha.2016.03.045>.
35. Ramakrishnan MS, Yu Y, VanderBeek BL. Association of visit adherence and visual acuity in patients with neovascular age-related macular degeneration: secondary analysis of the comparison of age-related macular degeneration treatment trial. *JAMA Ophthalmol.* 2020;138:237–242. <https://doi.org/10.1001/jamaophthalmol.2019.4577>.
36. Khanani AM, Aziz AA, Khan H, et al. The real-world efficacy and safety of faricimab in neovascular age-related macular degeneration: the TRUCKEE study—6 month results. *Eye (Lond).* 2023;37:3574–3581. <https://doi.org/10.1038/s41433-023-02553-5>.
37. Tro NJ. *Introductory Chemistry Essentials*. 5th ed. Boston, MA: Pearson; 2014.
38. Ho AC, Busbee BG, Regillo CD, et al. Twenty-four-month efficacy and safety of 0.5 mg or 2.0 mg ranibizumab in patients with subfoveal neovascular age-related macular degeneration. *Ophthalmology.* 2014;121:2181–2192. <https://doi.org/10.1016/j.ophtha.2014.05.009>.
39. Fagiani E, Christofori G. Angiopoietins in angiogenesis. *Cancer Lett.* 2013;328:18–26. <https://doi.org/10.1016/j.canlet.2012.08.018>.